

# On the homogeneity of SnIa absolute magnitude in the Pantheon+ sample

Leandros Perivolaropoulos<sup>1,\*</sup> and Foteini Skara<sup>1,†</sup>

<sup>1</sup>*Department of Physics, University of Ioannina, GR-45110, Ioannina, Greece*

(Dated: January 4, 2023)

We test the homogeneity of the Pantheon+ sample with respect to the intrinsic absolute luminosity  $M = m_{Bi} - \mu_i$  of the type Ia supernovae (SnIa) in Cepheid hosts and in the Hubble flow. Here,  $m_{Bi}$  is the corrected/standardized SnIa apparent magnitude and  $\mu_i$  is the  $i^{th}$  SnIa distance modulus obtained either from Cepheids (for SnIa in Cepheid hosts) or from the parametrized Hubble expansion rate  $H(z)$  (for the rest of the SnIa). When  $M$  is allowed to take a single value in the context of flat  $\Lambda$ CDM cosmological background  $H(z)$ , we find the expected best fit values  $M = -19.25 \pm 0.03$ ,  $\Omega_{0m} = 0.33 \pm 0.02$ ,  $H_0 = (73.4 \pm 1) \text{ km s}^{-1} \text{ Mpc}^{-1}$  consistent with the original analysis of Brout et al. When we introduce a new degree of freedom allowing  $M$  to take two values, one ( $M_<$ ) for nearby SnIa (distance  $d_i < d_{crit}$ ,  $\mu_i < 5 \log_{10}(d_{crit}/\text{Mpc}) + 25$ ) and one ( $M_>$ ) for more distant SnIa, we find a  $2-3\sigma$  tension between the two best fit values of  $M_> = -19.215 \pm 0.03$  and  $M_< = -19.362 \pm 0.05$  for  $d_{crit} \simeq 20 \text{ Mpc}$ . However, in contrast to the pure SH0ES data, this degree of freedom does not affect significantly the best fit values for the cosmological parameters  $H_0$  and  $\Omega_{0m}$  obtained from Pantheon+, for any value of  $d_{crit}$ , due to the dominant effects of the covariance matrix. When  $M$  is allowed to take distinct values  $M_i$  for each SnIa in Cepheid hosts we find using a KS test, that the  $M_i$  of nearby SnIa ( $d_i < 20 \text{ Mpc}$ ) have less than 2.5% probability to have been drawn from the same probability distribution as the  $M_i$  of more distant SnIa ( $d > 20 \text{ Mpc}$ ). These results constitute hints of inhomogeneities in the Pantheon+ sample which could be due to large statistical fluctuations, unaccounted systematic effects or new physics.

## I. INTRODUCTION

The value of the Hubble constant  $H_0$  measured by direct local measurements based mainly on Type Ia supernovae (SnIa) standard candles calibrated using distance ladder methods is at  $5\sigma$  tension with the corresponding value of  $H_0$  measured indirectly using the sound horizon at last scattering as a standard ruler. This discrepancy constitutes one of the main challenges for the standard cosmological model  $\Lambda$ CDM known as the Hubble tension.

The most precise direct method for measuring the Hubble constant is based on observations of SnIa calibrated with Cepheid variable stars in galaxies that host both Cepheid variable stars and SnIa. Cepheids in turn are calibrated using geometric methods (e.g. parallax) in the Milky Way and other nearby anchor galaxies. This is the distance ladder method for the direct measurement of  $H_0$ .

Such a distance ladder approach has been implemented recently by the SH0ES team (Supernovae and H0 for the Equation of State of dark energy) and has lead to a best fit value  $H_0^{R21} = 73.04 \pm 1.04 \text{ km s}^{-1} \text{ Mpc}^{-1}$  [1]. The corresponding indirect measurement of  $H_0$  using the sound horizon at recombination as a standard ruler measured by the CMB perturbations angular power spectrum under the assumption of the validity of the standard cosmological model  $\Lambda$ CDM (inverse distance ladder approach) has lead to an even more precise value of  $H_0^{P18} = 67.36 \pm 0.54 \text{ km s}^{-1} \text{ Mpc}^{-1}$  [2] (see also Refs. [3–12] for relevant recent reviews). The  $5\sigma$  discrepancy

(tension) between these two very precise measurements of  $H_0$  indicates that most probably at least one of them is not accurate because the assumptions on which it is based are not valid.

The local direct measurement of SH0ES is consistent with a wide range of other less precise local measurements of  $H_0$  using alternative SnIa calibrators [13–16], gravitational lensing [17–20], gravitational waves [21–25], gamma-ray bursts as standardizable candles [26–30], quasars as distant standard candles [31], type II supernovae [32, 33],  $\gamma$ -ray attenuation [34] etc. (for recent reviews see Refs. [3, 5]).

The SH0ES measurement relies on the following assumptions:

- The measurements of the properties (period, metallicity) and luminosities of Cepheid calibrators and SnIa are accurate and free of unaccounted systematic errors.
- The modeling and physical laws involved in the calibration of Cepheids and SnIa in the three rungs of the distance ladder are accurate and well understood.

A recent analysis by the authors [35] has indicated that a simple variation of the Cepheid/SnIa modeling in the SH0ES analysis introducing a single new degree of freedom can potentially modify the best fit value of  $H_0$  in such a way that it may become consistent with the corresponding inverse distance ladder measurement. This new degree of freedom allows for a transition of the SnIa calibrated and corrected intrinsic luminosity (absolute magnitude  $M$ ) at some distance or redshift. It would therefore be interesting to introduce this new degree of freedom in the new extended Pantheon+ sample

\* [leandros@uoi.gr](mailto:leandros@uoi.gr)

† [f.skara@uoi.gr](mailto:f.skara@uoi.gr)

[36–38] which includes many more SNIa than the local SH0ES Cepheid+SNIa sample, to investigate if this degree of freedom is excited by the data.

The Pantheon+ SNIa luminosity sample [36–38] provides distance moduli derived from 1701 light curves of 1550 SNIa in a redshift range  $z \in [0.001, 2.26]$  compiled across 18 different surveys. This sample is significantly improved over the first Pantheon sample of 1048 SNIa, especially at low redshift ( $z$ ).

During the past few months when the Pantheon+ sample has been publicly available, a wide range of studies have investigated various aspects of it. In particular, the following aspects of Pantheon+ have been investigated: its consistency with the cosmological principle [39, 40], the self-consistency level of its covariance [41], its consistency with standard electromagnetism and gravity [42], the constraints it can provide on modified gravity and generalized dark energy [36, 43–46], the constraints it can provide on early dark energy [47, 48], the constraints it can provide on the start of cosmic acceleration [49], the constraints on possible modification of physics at recombination (e.g. electron mass variation) [50], the identification of possible change of the best fit value of  $H_0$  when different redshift bins are considered [51, 52], the effects of binning on its data [53, 54], its consistency with BAO+BBN data [55], the constraints it implies on generalization of the Hubble law [56] etc.

One novel feature of Pantheon+ is that it may be used to infer  $H_0$  in addition to cosmological parameters. This is due to the fact that it includes the distance moduli of SNIa in Cepheid hosts as obtained directly from the distance ladder analysis of the SH0ES. It also includes the covariance of these SNIa with the SNIa in the Hubble flow. The estimate of  $H_0$  was not possible in the first Pantheon sample because of the degeneracy between  $H_0$  and SNIa absolute magnitude  $M$ . The inclusion of both the apparent magnitude  $m_B$  and the distance modulus from Cepheids  $\mu_{Ceph}$  for SNIa in Cepheid hosts allows the independent determination of the absolute magnitude  $M = m_B - \mu_{Ceph}$  which breaks the degeneracy between  $M$  and  $H_0$  thus allowing the independent determination of  $H_0$  through the Pantheon+ sample.

Due to the new features and data included in the Pantheon+ sample the following questions may be addressed:

- Is the best fit value of the SNIa absolute magnitude  $M$  consistent among various subsamples of the Pantheon+ sample?
- What is the effect of the introduction of new degrees of freedom (e.g. allowing for a change of  $M$ ) on the quality of fit and on the best fit values of  $H_0$  and cosmological parameters (e.g. matter density  $\Omega_{0m}$ )?

The goal of the present analysis is to address these questions focusing on the possible inhomogeneities of the standardized/corrected intrinsic luminosity (absolute magnitude) of the SNIa of the Pantheon+ sample. Investigations of possible inhomogeneities of other properties

of the SNIa (e.g. color or stretch parameters [57]) are also interesting but are beyond the scope of the present study.

The structure of this paper is the following: In the next section II we describe the data of the Pantheon+ sample that are relevant for our analysis and describe the method used for the fit of the cosmological parameters, the Hubble parameter  $H_0$  and the SNIa absolute magnitude  $M$ . We then implement this method and obtain the corresponding best fit parameter values for  $\Omega_{0m}$ ,  $H_0$  and  $M$  in the context of a  $\Lambda$ CDM background thus confirming the results of the original analysis of Brout et. al. [36] and verifying our implementation of the method described there. In section III, we generalize the model and the fitting method by allowing for a transition of the SNIa intrinsic luminosity  $M$  at some distance  $d_{crit}$  from a value  $M_<$  at distances  $d < d_{crit}$  to a value  $M_>$  at distances  $d > d_{crit}$ . We find the best fit parameter values for  $\Omega_{0m}$ ,  $H_0$   $M_<$  and  $M_>$  with their uncertainties and test the consistency between the best fit values of  $M_<$  and  $M_>$ . In section IV we discuss the statistical properties of the intrinsic luminosities  $M_i$  of SNIa in Cepheid hosts as obtained from the SNIa apparent magnitudes  $m_{Bi}$  and the Cepheid distance moduli  $\mu_i^{Ceph}$ . We check in particular the consistency of the statistical properties of the luminosities among different subsamples of the Pantheon+ sample. Finally in Section V we review our main results, discuss their implications and point out possible future extensions of our analysis.

## II. THE STANDARD ANALYSIS OF THE PANTHEON+ SAMPLE FOR $\Lambda$ CDM

The Pantheon+ sample is presented through a table (Pantheon+SH0ES.dat) with 1701 rows (plus a header) which includes the data relevant to 1701 SNIa light curves in 47 columns which are described at [this url](#). It also consists of a  $1701 \times 1701$  covariance matrix  $C_{\text{stat+syst}}$  which represents the covariance between SNIa due to systematic and statistical distance moduli uncertainties as described below. The relevant columns for our analysis are the following:

- **Column 3:** Hubble Diagram Redshift (with CMB and peculiar velocity corrections).
- **Columns 9–10:**  $m_B$  corrected/standardized SNIa apparent magnitude and its uncertainty as obtained from the diagonal of the covariance matrix.
- **Columns 11–12:**  $\mu = m_B - M_{Ceph}$  corrected/standardized distance moduli where the absolute SNIa magnitude  $M_{Ceph} = -19.253$  has been determined from SH0ES 2021 Cepheid host distances. Its uncertainty as obtained from the diagonal of the covariance matrix is included in column 12. Column 11 is superfluous as it is trivially obtained from column 9 by subtracting  $M_{Ceph}$ .

- **Column 13:**  $\mu_{Ceph}$  corrected/standardized distance moduli of the SnIa host as obtained from the SH0ES distance ladder analysis [1] in the context of the  $H_0$  distance ladder measurement. The uncertainty of  $\mu_{Ceph}$  is not included in this Table but it is incorporated in the covariance matrix. This column has entries only in the rows which correspond to SnIa in Cepheid hosts. The rest of the rows have an entry '-9' in this column.
- **Column 14:** Takes the value 1 if the SnIa of the row is in Cepheid host and 0 otherwise.

In this section we follow [36] and use the above described Pantheon+ data to constrain the Hubble parameter  $H_0 = 100 h \text{ km s}^{-1} \text{ Mpc}^{-1}$ , the SnIa absolute magnitude  $M$  and the matter density parameter  $\Omega_{0m}$  by minimizing a  $\chi^2$  likelihood:

$$\chi^2 = \vec{Q}^T \cdot (C_{\text{stat+syst}})^{-1} \cdot \vec{Q}, \quad (2.1)$$

where  $\vec{Q}$  is a vector with dimension 1701 and components which are usually defined as

$$Q_i = m_{Bi} - M - \mu_{\text{model}}(z_i), \quad (2.2)$$

where  $m_{Bi} - M = \mu_i$  is the distance modulus of the  $i^{th}$  SnIa and  $\mu_{\text{model}}(z_i)$  is the corresponding distance modulus as predicted by the assumed background cosmological model parametrization which in the present analysis is assumed to be  $\Lambda\text{CDM}$ . Thus we have

$$\mu_{\text{model}}(z_i) = 5 \log(d_L(z_i)/\text{Mpc}) + 25, \quad (2.3)$$

where the luminosity distance  $d_L(z)$  is

$$d_L(z) = (1+z)c \int_0^z \frac{dz'}{H(z')}, \quad (2.4)$$

where  $c$  is the speed of light and in a  $\Lambda\text{CDM}$  background

$$H(z) = H_0 \sqrt{\Omega_M(1+z)^3 + \Omega_\Lambda}. \quad (2.5)$$

The parameters  $M$  and  $H_0$  appear in Eqs. (2.1), (2.2) only through the combination  $\mathcal{M} \equiv M - 5 \log(H_0 \cdot \text{Mpc}/c)$  and therefore they are degenerate and can not be estimated separately. In order to break this degeneracy,  $M$  can be estimated separately using the distance ladder approach by calibrating SnIa using Cepheids as was done with previous Pantheon sample. In the Pantheon+ sample this degeneracy is broken within the analysis by modifying the definition of (2.2) to include the distance moduli of SnIa in Cepheid hosts which can constrain  $M$  independently. Thus the vector  $\vec{Q}$  in the likelihood definition (2.2) is modified as follows [36]

$$Q'_i = \begin{cases} m_{Bi} - M - \mu_i^{\text{Ceph}} & i \in \text{Cepheid hosts} \\ m_{Bi} - M - \mu_{\text{model}}(z_i) & \text{otherwise,} \end{cases} \quad (2.6)$$

where  $\mu_i^{\text{Ceph}}$  is the distance modulus of the Cepheid host of the  $i^{th}$  SnIa which is measured independently in the context of the distance ladder with Cepheid calibrators [1]. The novel feature of Pantheon+ is that the components  $Q'_i$  that correspond to SnIa in Cepheid hosts are now fully incorporated in the sample and correlated with the rest of the SnIa though the provided covariance matrix. Thus, the degeneracy between  $M$  and  $H_0$  is broken and the three parameters  $M$ ,  $H_0$  and  $\Omega_{0m}$  can be fit in the context of a  $\Lambda\text{CDM}$  background by minimizing

$$\chi'^2(M, H_0, \Omega_{0m}) = \vec{Q}'^T \cdot (C_{\text{stat+syst}})^{-1} \cdot \vec{Q}', \quad (2.7)$$

where  $C_{\text{stat+syst}}$  denotes the covariance matrix provided with the Pantheon+ data including both statistical and systematic uncertainties. We have obtained the best fit parameter values for  $M$ ,  $H_0$  and  $\Omega_{0m}$  and constructed the  $1\sigma$ – $3\sigma$  likelihood contours by minimizing  $\chi'^2$  of Eq. (2.7) using a simple Mathematica v12 code which is publicly available.

The uncertainties for each one of the three best fit parameters were obtained using the square roots of the diagonal elements of the parameter covariance matrix which is the inverse of the Fisher matrix defined as

$$F_{ij} = \frac{1}{2} \frac{\partial^2 \chi'^2(p_1, p_2, p_3)}{\partial p_i \partial p_j}, \quad (2.8)$$

where  $i, j = 1, 2, 3$  and the parameters  $p_1, p_2, p_3$  correspond to  $M$ ,  $h$  and  $\Omega_{0m}$ . We thus find

$$M = -19.25 \pm 0.03, \quad (2.9)$$

$$h = 0.734 \pm 0.01, \quad (2.10)$$

$$\Omega_{0m} = 0.333 \pm 0.018, \quad (2.11)$$

which is in excellent agreement with the best fit values for  $h$  and  $\Omega_{0m}$  reported in [36]. The corresponding parameter likelihood contours are the blue contours shown in Fig. 1.

At the minimum we also find  $\chi'^2_{\min} = 1522.98$  which corresponds to a  $\chi'^2$  per degree of freedom of about 0.9. This is less than 1 and may indicate a possible overestimation of the uncertainties in the covariance matrix as pointed out recently in Ref. [41].

### III. GENERALIZED ANALYSIS ALLOWING TRANSITION OF SNIA LUMINOSITY.

In order to test the homogeneity of the calibrated SnIa intrinsic luminosity, we now generalize the model of the previous section not by allowing more cosmological parameters but by allowing a change of the absolute magnitude at a distance  $d_{\text{crit}}$  such that the SnIa absolute magnitude is of the form

$$M = \begin{cases} M_< & d < d_{\text{crit}} \\ M_> & d > d_{\text{crit}}, \end{cases} \quad (3.1)$$

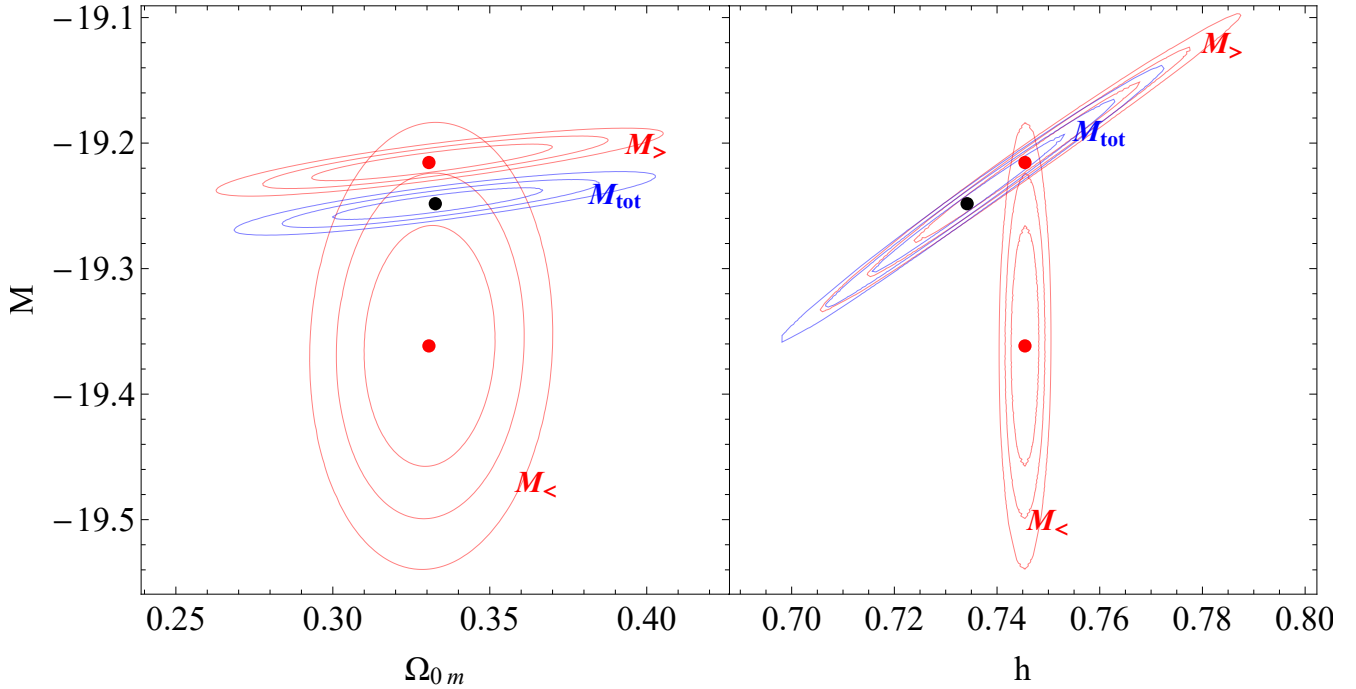


Figure 1. Blue contours: The  $1-3\sigma$  likelihood contours for the parameters  $M$ ,  $h$  and  $\Omega_{0m}$  in the context of a  $\Lambda$ CDM background. Red contours: The  $1-3\sigma$  likelihood contours for the parameters  $M_<$ ,  $M_>$ ,  $h$  and  $\Omega_{0m}$  in the context of a  $\Lambda$ CDM background in a model that allows for a transition of the SnIa absolute magnitude from a value  $M_<$  at distances  $d < 20Mpc$  to a value  $M_>$  at distances  $d > 20Mpc$ .

The magnitude transition critical distance  $d_{crit}$  may be associated with a critical distance modulus through the relation  $\mu_{crit} = 5\log(d_{crit}/Mpc) + 25$ . By introducing

this degree of freedom in  $\chi^2$  we obtain a generalized  $\chi''^2(M_<, M_>, h, \Omega_{0m})$  defined by using a vector  $\vec{Q}''$  of the form

$$Q''_i = \begin{cases} m_{Bi} - M_< - \mu_i^{\text{Cepheid}} & \text{iff } \mu_i^{\text{Cepheid}} < \mu_{crit}, \text{ and } i \in \text{Cepheid hosts} \\ m_{Bi} - M_> - \mu_i^{\text{Cepheid}} & \text{iff } \mu_i^{\text{Cepheid}} > \mu_{crit}, \text{ and } i \in \text{Cepheid hosts} \\ m_{Bi} - M_< - \mu_{\text{model}}(z_i) & \text{iff } \mu_i^{\text{Cepheid}} < \mu_{crit}, \text{ and } i \notin \text{Cepheid hosts} \\ m_{Bi} - M_> - \mu_{\text{model}}(z_i) & \text{iff } \mu_i^{\text{Cepheid}} > \mu_{crit}, \text{ and } i \notin \text{Cepheid hosts}, \end{cases} \quad (3.2)$$

in the expression (2.1) for  $\chi^2$ .

Previous studies [35, 58–60] have found hints of inhomogeneities of astrophysical properties including the parameters of the Tully-Fisher relation at a distance of about  $20Mpc$ .

In Ref. [35] it was also pointed out that if the SH0ES data are reanalyzed by allowing for a change of the SnIa absolute magnitude at  $d_{crit} = 50Mpc$  then the best fit value of the Hubble parameter shifts to a value almost identical with the inverse distance ladder best fit value albeit with significantly increased uncertainties. Motivated by these studies we first set  $d_{crit} = 50Mpc$  ( $\mu_{crit} = 31.5$ ) and minimize the generalized  $\chi''^2(M_<, M_>, h, \Omega_{0m})$ . We thus find the following best fit parameter values with the

corresponding  $1\sigma$  uncertainties

$$M_< = -19.25 \pm 0.03, \quad (3.3)$$

$$M_< = -19.23 \pm 0.05, \quad (3.4)$$

$$h = 0.742 \pm 0.02, \quad (3.5)$$

$$\Omega_{0m} = 0.332 \pm 0.018, \quad (3.6)$$

with no change of the quality of fit since  $\chi''^2_{min} = 1522.61$  ( $\Delta\chi''^2_{min} = -0.3$ ). Thus for  $d_{crit} = 50Mpc$  we find no hint of discrepancy between  $M_<$  and  $M_>$  and thus no inhomogeneity with respect to the SnIa intrinsic luminosities. In addition no significant change is observed in the best fit value of  $h$  in contrast to the corresponding result for the SH0ES data analysis where the same degree

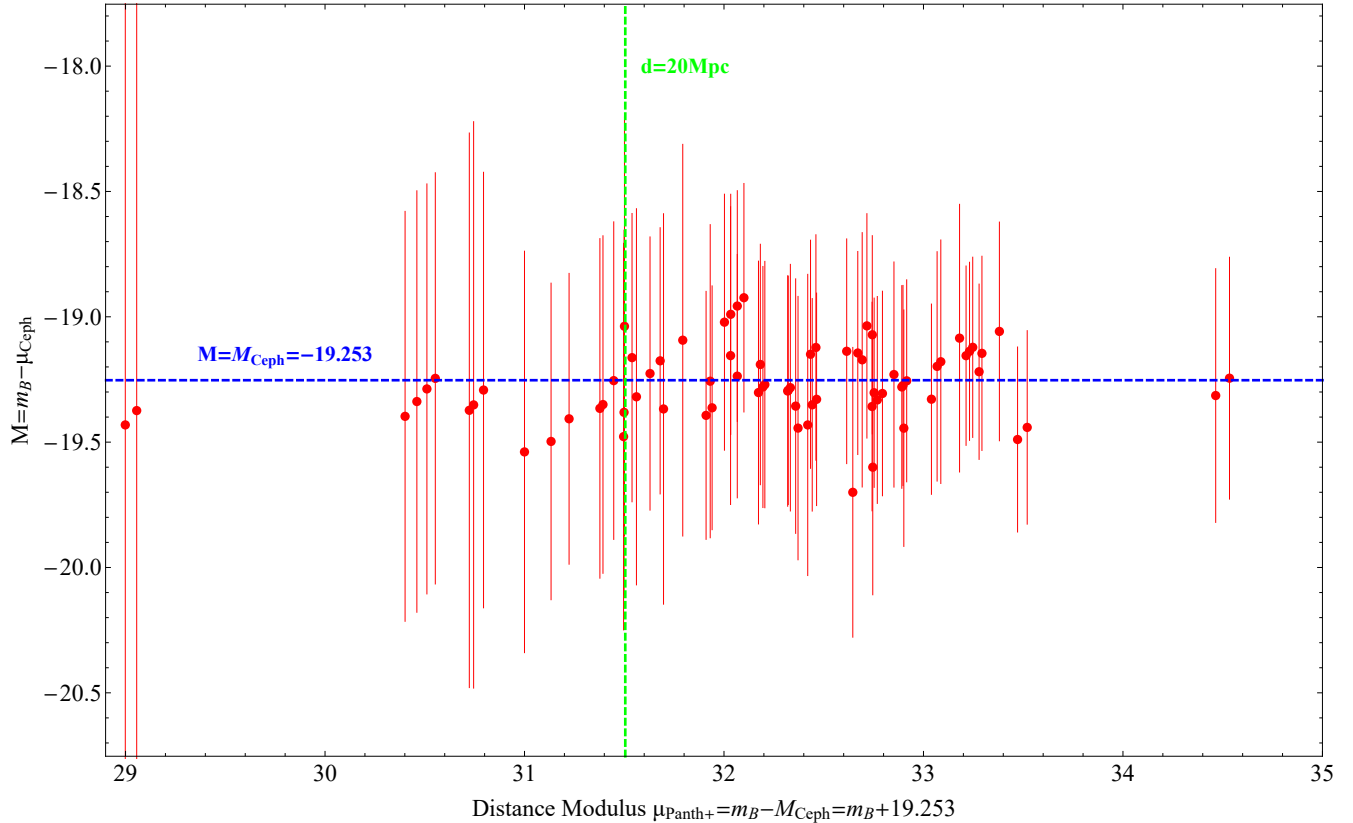


Figure 2. The absolute magnitudes of SnIa residing in Cepheid hosts. The best fit SnIa standardized and corrected absolute magnitude based on the SH0ES analysis is also shown (blue dashed line).

of freedom induced a shift in the best fit value of  $h$  to  $h = 0.67 \pm 0.04$ . This may be due to the small number of SnIa in Cepheid hosts for the  $M_>$  bin (4 SnIa) combined with the much larger number of SnIa in the Hubble flow bin for the Pantheon+ sample and the much more extensive covariance matrix. Similarly, for other values of  $d_{crit}$  no significant change is found for the best fit values of the parameters  $h$  and  $\Omega_{0m}$ . However, for  $d_{crit} \simeq 20 Mpc$  we find a mild discrepancy between the best fit values of  $M_<$  and  $M_>$ .

In particular, for  $d_{crit} = 20 Mpc$  we find the following best fit parameter values with the corresponding  $1\sigma$  uncertainties

$$M_< = -19.362 \pm 0.05, \quad (3.7)$$

$$M_< = -19.215 \pm 0.03, \quad (3.8)$$

$$h = 0.745 \pm 0.01, \quad (3.9)$$

$$\Omega_{0m} = 0.331 \pm 0.018, \quad (3.10)$$

with a significant improvement of the quality of fit since  $\chi''_{min}^2 = 1513.3$  ( $\Delta\chi''_{min}^2 = -9.7$ ) corresponding to reduction of the Akaike Information Criterion (AIC) by  $\Delta AIC = -7.7$  (for a single additional parameter). The corresponding likelihood contours for these parameters are shown in Fig. 2 (red contours for  $M_<$  and  $M_>$ ).

Thus for  $d_{crit} = 20 Mpc$  we find hints of discrepancy between  $M_<$  and  $M_>$  at a  $2-3\sigma$  level and thus inhomogeneity with respect to the SnIa intrinsic luminosities.

However, no significant change is observed in the best fit value of  $h$ . This was also the case for the SH0ES data analysis for the same value of  $d_{crit}$ , where the same degree of freedom induced no significant shift in the best fit value of  $h$  [35] even though hints of discrepancy between  $M_<$  and  $M_>$  were observed at similar  $d_{crit}$  albeit at lower statistical significance (see e.g. Figs. 8, 9 of Ref. [35]).

#### IV. STATISTICAL PROPERTIES OF SNIA INTRINSIC LUMINOSITIES.

In this section we further investigate the hints for inhomogeneity derived in the previous section from the full Pantheon+ sample. We thus focus on the particular subset of the Pantheon+ sample that corresponds to SnIa in Cepheid hosts and investigate the statistical properties of their individual absolute magnitudes. The measured absolute magnitude  $M_i$  of individual SnIa in Cepheid hosts can be directly obtained from the Pantheon+ data as

$$M_i = m_{Bi} - \mu_i^{\text{Ceph}} \quad (4.1)$$

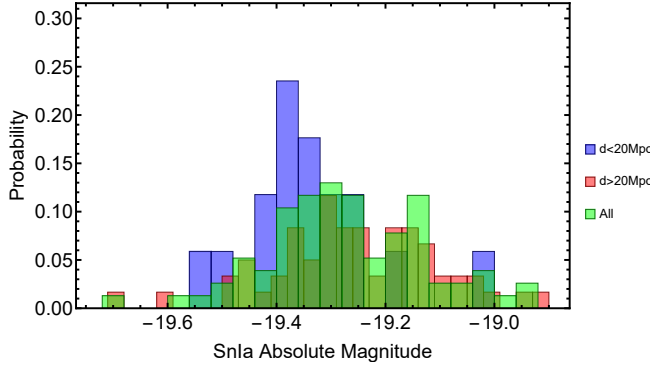


Figure 3. The probability distribution histogram of the absolute magnitudes each SNIa subsample (Nearby subsample  $M_s^<$ : dark blue columns, Distant subsample  $M_s^>$ : red columns, Full sample of SNIa in Cepheid hosts: green columns)

i.e. by subtracting column 13 from column 9 for those entries where column 14 is 1<sup>1</sup>. In Fig. 2 we show a plot of the measured  $M_i$  for SNIa in Cepheid hosts vs the SNIa distance moduli  $\mu_{Pantheon+} = m_{Bi} - M_{Ceph}$  (column 9) as obtained from the measured apparent magnitudes and the best fit value of  $M$  from SH0ES ( $M_{Ceph} = -19.253$ , blue dashed line). As shown in Fig. 2, SNIa at distances  $d < 20Mpc$  appear to be systematically more luminous (lower  $M_i$ ) than the rest of the SNIa since almost all are below the blue dashed line corresponding to  $M_{Ceph}$ <sup>2</sup>.

In order to compare the statistical properties of the  $M_i$  subsample with  $d < 20Mpc$  ( $M_s^<$ ) with the corresponding distant subsample with  $d > 20Mpc$  ( $M_s^>$ ) we show in Fig. 3 the probability distribution histogram of each subsample ( $M_s^<$ : dark blue columns,  $M_s^>$ : red columns, Full sample: green columns). As expected from Fig. 2 the probability distributions for the two subsamples differ significantly with  $M_s^<$  being significantly skewed towards lower  $M$  values (brighter SNIa).

The statistical difference between the two subsamples may be quantified using a Kolmogorov-Smirnov test. Based on this test, the null hypothesis that the two subsamples have been drawn from the same probability distribution is rejected at the 2.5% level. In fact the probability that the two subsamples have been drawn from the same probability distribution is 2.2%. This result further amplifies the evidence for inhomogeneities in the SNIa corrected intrinsic luminosities of the Pantheon+ sample. This inhomogeneity could be due to either a large statistical fluctuation in the context of the standard model, or to an unaccounted systematic effect or to

a physics transition that has occurred at a distance of about  $20Mpc$  (about 70Myrs ago) [61, 62].

## V. CONCLUSION-DISCUSSION

We have tested the internal consistency of the Pantheon+ sample with respect to the SNIa standardized and corrected intrinsic luminosity. We have allowed for a change of the SNIa absolute magnitude at  $d_{crit} = 20Mpc$  from  $M_<$  at low distances (late times) to  $M_>$  at high distances (early times). We found that such a change is favored by the Pantheon+ data leading to a reduction of  $\chi^2$  by  $\Delta\chi^2_{min} = -9.7$ . This corresponds to reduction of the Akaike Information Criterion (AIC) by  $\Delta AIC = -7.7$  (for a single additional parameter). Such a reduction provides strong evidence that the model where a change of  $M$  is preferred by the Pantheon+ data over the baseline model with a single value for  $M$ . This conclusion is further amplified by the fact that the best fit value of  $M_<$  is in discrepancy with the best fit value of  $M_>$  at a level of more than  $2\sigma$ . In addition, a Kolmogorov-Smirnov test has indicated that the probability that the absolute magnitudes  $M_i$  of SNIa in Cepheid hosts at distances  $d < 20Mpc$  are drawn from the same distribution as the  $M_i$  of SNIa at hosts with  $d > 20Mpc$  is less than 2.5%. These results constitute evidence for a possible inhomogeneity of the SNIa intrinsic luminosities of Pantheon+ sample with probability more than 95%. However, even if this inhomogeneity manifests itself by the introduction of a new degree of freedom in the analysis (replacing  $M$  by  $M_<$  and  $M_>$ ), the best fit values of the cosmological parameters  $\Omega_{0m}$  and  $H_0$  are not significantly affected. Notice however, that the best fit value  $M_< = -19.362 \pm 0.05$  of low the distance SNIa absolute magnitude is fully consistent with the inverse distance ladder best fit value  $M = -19.4 \pm 0.027$  [61].

The demonstrated presence of possible inhomogeneities in the Pantheon+ sample may have implications for other calibration parameters like the color and stretch parameters. It would therefore be of interest to extend the present analysis in such directions by testing the homogeneity of the Pantheon+ sample with respect to possible differences of the best fit values of such parameters when these are allowed to change among different subsamples of the full Pantheon+ sample. Hints for such inhomogeneities from the first Pantheon sample have been already reported [57]. The corresponding effect on the best fit values of cosmological parameters when such new degrees of freedom are allowed would also be an interesting extension of the present analysis.

<sup>1</sup> The uncertainty of each  $M_i$  is obtained from the corresponding entries of columns 10 and 13 only for plotting purposes as it will not be used in the statistical analysis of this section.

<sup>2</sup> A similar trend appears for the four furthest SNIa with  $d > 50Mpc$  even though this is much less significant statistically. This is the origin of the effects observed in [35].

## NUMERICAL ANALYSIS FILES

The numerical files for the reproduction of the figures can be found [this Github repository under the MIT](#)

license.

## ACKNOWLEDGMENTS

This project was supported by the Hellenic Foundation for Research and Innovation (H.F.R.I.), under the "First

call for H.F.R.I. Research Projects to support Faculty members and Researchers and the procurement of high-cost research equipment Grant" (Project Number: 789).

---

[1] Adam G. Riess *et al.*, "A Comprehensive Measurement of the Local Value of the Hubble Constant with  $1 \text{ km s}^{-1} \text{ Mpc}^{-1}$  Uncertainty from the Hubble Space Telescope and the SH0ES Team," *Astrophys. J. Lett.* **934**, L7 (2022), [arXiv:2112.04510 \[astro-ph.CO\]](https://arxiv.org/abs/2112.04510).

[2] N. Aghanim *et al.* (Planck), "Planck 2018 results. VI. Cosmological parameters," *Astron. Astrophys.* **641**, A6 (2020), [Erratum: *Astron. Astrophys.* 652, C4 (2021)], [arXiv:1807.06209 \[astro-ph.CO\]](https://arxiv.org/abs/1807.06209).

[3] Leandros Perivolaropoulos and Foteini Skara, "Challenges for  $\Lambda$ CDM: An update," *New Astron. Rev.* **95** (2022), 10.1016/j.newar.2022.101659, [arXiv:2105.05208 \[astro-ph.CO\]](https://arxiv.org/abs/2105.05208).

[4] Elcio Abdalla *et al.*, "Cosmology intertwined: A review of the particle physics, astrophysics, and cosmology associated with the cosmological tensions and anomalies," *JHEAp* **34**, 49–211 (2022), [arXiv:2203.06142 \[astro-ph.CO\]](https://arxiv.org/abs/2203.06142).

[5] Eleonora Di Valentino, Olga Mena, Supriya Pan, Luca Visinelli, Weiqiang Yang, Alessandro Melchiorri, David F. Mota, Adam G. Riess, and Joseph Silk, "In the realm of the Hubble tension—a review of solutions," *Class. Quant. Grav.* **38**, 153001 (2021), [arXiv:2103.01183 \[astro-ph.CO\]](https://arxiv.org/abs/2103.01183).

[6] Paul Shah, Pablo Lemos, and Ofer Lahav, "A buyer's guide to the Hubble constant," *Astron. Astrophys. Rev.* **29**, 9 (2021), [arXiv:2109.01161 \[astro-ph.CO\]](https://arxiv.org/abs/2109.01161).

[7] Lloyd Knox and Marius Millea, "The Hubble Hunter's Guide," (2019), [arXiv:1908.03663 \[astro-ph.CO\]](https://arxiv.org/abs/1908.03663).

[8] Sunny Vagnozzi, "New physics in light of the  $H_0$  tension: an alternative view," *Phys. Rev. D* **102**, 023518 (2020), [arXiv:1907.07569 \[astro-ph.CO\]](https://arxiv.org/abs/1907.07569).

[9] Mustapha Ishak, "Testing General Relativity in Cosmology," *Living Rev. Rel.* **22**, 1 (2019), [arXiv:1806.10122 \[astro-ph.CO\]](https://arxiv.org/abs/1806.10122).

[10] Edvard Mörtsell and Suhail Dhawan, "Does the Hubble constant tension call for new physics?" *JCAP* **1809**, 025 (2018), [arXiv:1801.07260 \[astro-ph.CO\]](https://arxiv.org/abs/1801.07260).

[11] Dragan Huterer and Daniel L Shafer, "Dark energy two decades after: Observables, probes, consistency tests," *Rept. Prog. Phys.* **81**, 016901 (2018), [arXiv:1709.01091 \[astro-ph.CO\]](https://arxiv.org/abs/1709.01091).

[12] Jose Luis Bernal, Licia Verde, and Adam G. Riess, "The trouble with  $H_0$ ," *JCAP* **1610**, 019 (2016), [arXiv:1607.05617 \[astro-ph.CO\]](https://arxiv.org/abs/1607.05617).

[13] Wendy L. Freedman, "Measurements of the Hubble Constant: Tensions in Perspective," (2021), [arXiv:2106.15656 \[astro-ph.CO\]](https://arxiv.org/abs/2106.15656).

[14] Adrià Gómez-Valent and Luca Amendola, " $H_0$  from cosmic chronometers and Type Ia supernovae, with Gaussian Processes and the novel Weighted Polynomial Regression method," *JCAP* **04**, 051 (2018), [arXiv:1802.01505 \[astro-ph.CO\]](https://arxiv.org/abs/1802.01505).

[15] D.W. Pesce *et al.*, "The Megamaser Cosmology Project. XIII. Combined Hubble constant constraints," *Astrophys. J. Lett.* **891**, L1 (2020), [arXiv:2001.09213 \[astro-ph.CO\]](https://arxiv.org/abs/2001.09213).

[16] Wendy L. Freedman, Barry F. Madore, Taylor Hoyt, In Sung Jang, Rachael Beaton, Myung Gyoong Lee, Andrew Monson, Jill Neeley, and Jeffrey Rich, "Calibration of the Tip of the Red Giant Branch (TRGB)," (2020), [arXiv:2002.01550 \[astro-ph.GA\]](https://arxiv.org/abs/2002.01550).

[17] Kenneth C. Wong *et al.*, "H0LiCOW – XIII. A 2.4 per cent measurement of  $H_0$  from lensed quasars:  $5.3\sigma$  tension between early- and late-Universe probes," *Mon. Not. Roy. Astron. Soc.* **498**, 1420–1439 (2020), [arXiv:1907.04869 \[astro-ph.CO\]](https://arxiv.org/abs/1907.04869).

[18] Geoff C. F. Chen *et al.*, "A SHARP view of H0LiCOW:  $H_0$  from three time-delay gravitational lens systems with adaptive optics imaging," *Mon. Not. Roy. Astron. Soc.* **490**, 1743–1773 (2019), [arXiv:1907.02533 \[astro-ph.CO\]](https://arxiv.org/abs/1907.02533).

[19] S. Birrer *et al.*, "TDCOSMO - IV. Hierarchical time-delay cosmography – joint inference of the Hubble constant and galaxy density profiles," *Astron. Astrophys.* **643**, A165 (2020), [arXiv:2007.02941 \[astro-ph.CO\]](https://arxiv.org/abs/2007.02941).

[20] S. Birrer *et al.*, "H0LiCOW - IX. Cosmographic analysis of the doubly imaged quasar SDSS 1206+4332 and a new measurement of the Hubble constant," *Mon. Not. Roy. Astron. Soc.* **484**, 4726 (2019), [arXiv:1809.01274 \[astro-ph.CO\]](https://arxiv.org/abs/1809.01274).

[21] M. Fishbach *et al.* (LIGO Scientific, Virgo), "A Standard Siren Measurement of the Hubble Constant from GW170817 without the Electromagnetic Counterpart," *Astrophys. J. Lett.* **871**, L13 (2019), [arXiv:1807.05667 \[astro-ph.CO\]](https://arxiv.org/abs/1807.05667).

[22] Kenta Hotokezaka, Ehud Nakar, Ore Gottlieb, Samaya Nissanke, Kento Masuda, Gregg Hallinan, Kunal P. Mooley, and Adam. T. Deller, "A Hubble constant measurement from superluminal motion of the jet in GW170817," *Nature Astron.* **3**, 940–944 (2019), [arXiv:1806.10596 \[astro-ph.CO\]](https://arxiv.org/abs/1806.10596).

[23] B. P. Abbott *et al.* (LIGO Scientific, Virgo, 1M2H, Dark Energy Camera GW-E, DES, DLT40, Las Cumbres Observatory, VINROUGE, MASTER), "A gravitational-wave standard siren measurement of the Hubble constant," *Nature* **551**, 85–88 (2017), [arXiv:1710.05835 \[astro-ph.CO\]](https://arxiv.org/abs/1710.05835).

[24] A. Palmese *et al.* (DES), "A statistical standard siren measurement of the Hubble constant from the LIGO/Virgo gravitational wave compact object merger

GW190814 and Dark Energy Survey galaxies,” *Astrophys. J. Lett.* **900**, L33 (2020), arXiv:2006.14961 [astro-ph.CO].

[25] M. Soares-Santos *et al.* (DES, LIGO Scientific, Virgo), “First Measurement of the Hubble Constant from a Dark Standard Siren using the Dark Energy Survey Galaxies and the LIGO/Virgo Binary-Black-hole Merger GW170814,” *Astrophys. J. Lett.* **876**, L7 (2019), arXiv:1901.01540 [astro-ph.CO].

[26] Shulei Cao, Maria Dainotti, and Bharat Ratra, “Standardizing Platinum Dainotti-correlated gamma-ray bursts, and using them with standardized Amati-correlated gamma-ray bursts to constrain cosmological model parameters,” *Mon. Not. Roy. Astron. Soc.* **512**, 439–454 (2022), arXiv:2201.05245 [astro-ph.CO].

[27] Shulei Cao, Maria Dainotti, and Bharat Ratra, “Gamma-ray burst data strongly favor the three-parameter fundamental plane (Dainotti) correlation relation over the two-parameter one,” (2022), 10.1093/mnras/stac2170, arXiv:2204.08710 [astro-ph.CO].

[28] Maria Giovanna Dainotti, Giuseppe Sarracino, and Salvatore Capozziello, “Gamma-Ray Bursts, Supernovae Ia and Baryon Acoustic Oscillations: a binned cosmological analysis,” (2022), 10.1093/pasj/psac057, arXiv:2206.07479 [astro-ph.CO].

[29] Maria Giovanna Dainotti, Via Nielson, Giuseppe Sarracino, Enrico Rinaldi, Shigehiro Nagataki, Salvatore Capozziello, Oleg Y. Gnedin, and Giada Bargiacchi, “Optical and X-ray GRB Fundamental Planes as cosmological distance indicators,” *Mon. Not. Roy. Astron. Soc.* **514**, 1828–1856 (2022), arXiv:2203.15538 [astro-ph.CO].

[30] Maria Giovanna Dainotti, Vincenzo Fabrizio Cardone, Ester Piedipalumbo, and Salvatore Capozziello, “Slope evolution of GRB correlations and cosmology,” *Mon. Not. Roy. Astron. Soc.* **436**, 82 (2013), arXiv:1308.1918 [astro-ph.HE].

[31] Guido Risaliti and Elisabeta Lusso, “Cosmological constraints from the Hubble diagram of quasars at high redshifts,” *Nature Astron.* **3**, 272–277 (2019), arXiv:1811.02590 [astro-ph.CO].

[32] T. de Jaeger, L. Galbany, A. G. Riess, B. E. Stahl, B. J. Shappee, A. V. Filippenko, and W. Zheng, “A 5% measurement of the Hubble constant from Type II supernovae,” (2022), 10.1093/mnras/stac1661, arXiv:2203.08974 [astro-ph.CO].

[33] T. de Jaeger, B.E. Stahl, W. Zheng, A.V. Filippenko, A.G. Riess, and L. Galbany, “A measurement of the Hubble constant from Type II supernovae,” (2020), 10.1093/mnras/staa1801, arXiv:2006.03412 [astro-ph.CO].

[34] Alberto Domínguez, Radoslaw Wojtak, Justin Finke, Marco Ajello, Kari Helgason, Francisco Prada, Abhishek Desai, Vaidehi Paliya, Lea Marcotulli, and Dieter Hartmann, “A new measurement of the Hubble constant and matter content of the Universe using extragalactic background light  $\gamma$ -ray attenuation,” (2019), 10.3847/1538-4357/ab4a0e, arXiv:1903.12097 [astro-ph.CO].

[35] Leandros Perivolaropoulos and Foteini Skara, “A Reanalysis of the Latest SH0ES Data for  $H_0$ : Effects of New Degrees of Freedom on the Hubble Tension,” *Universe* **8**, 502 (2022), arXiv:2208.11169 [astro-ph.CO].

[36] Dillon Brout *et al.*, “The Pantheon+ Analysis: Cosmological Constraints,” *Astrophys. J.* **938**, 110 (2022), arXiv:2202.04077 [astro-ph.CO].

[37] Dan Scolnic *et al.*, “The Pantheon+ Analysis: The Full Data Set and Light-curve Release,” *Astrophys. J.* **938**, 113 (2022), arXiv:2112.03863 [astro-ph.CO].

[38] Dillon Brout *et al.*, “The Pantheon+ Analysis: SuperCalfragilistic Cross Calibration, Retrained SALT2 Light-curve Model, and Calibration Systematic Uncertainty,” *Astrophys. J.* **938**, 111 (2022), arXiv:2112.03864 [astro-ph.CO].

[39] Jessica A. Cowell, Suhail Dhawan, and Hayley J. Macpherson, “Potential signature of a quadrupolar Hubble expansion in Pantheon+ supernovae,” (2022), arXiv:2212.13569 [astro-ph.CO].

[40] Francesco Sorrenti, Ruth Durrer, and Martin Kunz, “The Dipole of the Pantheon+SH0ES Data,” (2022), arXiv:2212.10328 [astro-ph.CO].

[41] Ryan Keeley, Arman Shafieloo, and Benjamin L’Huillier, “An Analysis of Variance of the Pantheon+ Dataset: Systematics in the Covariance Matrix?” (2022), arXiv:2212.07917 [astro-ph.CO].

[42] Giuseppe Sarracino, Alessandro D. A. M. Spallicci, and Salvatore Capozziello, “Investigating dark energy by electromagnetic frequency shifts II: the Pantheon+ sample,” *Eur. Phys. J. Plus* **137**, 1386 (2022), arXiv:2211.11438 [astro-ph.CO].

[43] Vivian Poulin, José Luis Bernal, Ely Kovetz, and Marc Kamionkowski, “The Sigma-8 Tension is a Drag,” (2022), arXiv:2209.06217 [astro-ph.CO].

[44] Deng Wang, “Pantheon+ constraints on dark energy and modified gravity: An evidence of dynamical dark energy,” *Phys. Rev. D* **106**, 063515 (2022), arXiv:2207.07164 [astro-ph.CO].

[45] S. A. Narawade and B. Mishra, “Phantom cosmological model with observational constraints in  $f(Q)$  gravity,” (2022), arXiv:2211.09701 [gr-qc].

[46] Reginald Christian Bernardo, Daniela Grandón, Jackson Levi Said, and Víctor H. Cárdenas, “Dark energy by natural evolution: Constraining dark energy using Approximate Bayesian Computation,” (2022), arXiv:2211.05482 [astro-ph.CO].

[47] Marc Kamionkowski and Adam G. Riess, “The Hubble Tension and Early Dark Energy,” (2022), arXiv:2211.04492 [astro-ph.CO].

[48] Théo Simon, Pierre Zhang, Vivian Poulin, and Tristan L. Smith, “Updated constraints from the effective field theory analysis of BOSS power spectrum on Early Dark Energy,” (2022), arXiv:2208.05930 [astro-ph.CO].

[49] David Dahya and Deepak Jain, “Revisiting the epoch of cosmic acceleration,” (2022), arXiv:2212.04751 [astro-ph.CO].

[50] Nanoom Lee, Yacine Ali-Haïmoud, Nils Schöneberg, and Vivian Poulin, “What it takes to solve the Hubble tension through modifications of cosmological recombination,” (2022), arXiv:2212.04494 [astro-ph.CO].

[51] X. D. Jia, J. P. Hu, and F. Y. Wang, “The evidence for a decreasing trend of Hubble constant,” (2022), arXiv:2212.00238 [astro-ph.CO].

[52] Wang-Wei Yu, Li Li, and Shao-Jiang Wang, “First detection of the Hubble variation correlation and its scale dependence,” (2022), arXiv:2209.14732 [astro-ph.CO].

[53] Eoin Ó. Colgáin, M. M. Sheikh-Jabbari, and Rance Solomon, “High Redshift  $\Lambda$ CDM Cosmology: To Bin or not to Bin?” (2022), arXiv:2211.02129 [astro-ph.CO].

- [54] Deng Wang, “Pantheon+ tomography and Hubble tension,” (2022), [arXiv:2207.10927 \[astro-ph.CO\]](https://arxiv.org/abs/2207.10927).
- [55] Nils Schöneberg, Licia Verde, Héctor Gil-Marín, and Samuel Brieden, “BAO+BBN revisited — growing the Hubble tension with a 0.7 km/s/Mpc constraint,” *JCAP* **11**, 039 (2022), [arXiv:2209.14330 \[astro-ph.CO\]](https://arxiv.org/abs/2209.14330).
- [56] Deng Wang, “Testing the Hubble law with Pantheon+,” (2022), [arXiv:2208.07271 \[astro-ph.CO\]](https://arxiv.org/abs/2208.07271).
- [57] Radosław Wojtak and Jens Hjorth, “Intrinsic tension in the supernova sector of the local Hubble constant measurement and its implications,” (2022), [10.1093/mnras/stac1878](https://doi.org/10.1093/mnras/stac1878), [arXiv:2206.08160 \[astro-ph.CO\]](https://arxiv.org/abs/2206.08160).
- [58] George Alestas, Ioannis Antoniou, and Leandros Perivolaropoulos, “Hints for a gravitational constant transition in Tully-Fisher data,” (2021), [arXiv:2104.14481 \[astro-ph.CO\]](https://arxiv.org/abs/2104.14481).
- [59] Leandros Perivolaropoulos and Foteini Skara, “Hubble tension or a transition of the Cepheid SnIa calibrator parameters?” *Phys. Rev. D* **104**, 123511 (2021), [arXiv:2109.04406 \[astro-ph.CO\]](https://arxiv.org/abs/2109.04406).
- [60] Leandros Perivolaropoulos, “Is the Hubble Crisis Connected with the Extinction of Dinosaurs?” *Universe* **8**, 263 (2022), [arXiv:2201.08997 \[astro-ph.EP\]](https://arxiv.org/abs/2201.08997).
- [61] Valerio Marra and Leandros Perivolaropoulos, “A rapid transition of  $G_{\text{eff}}$  at  $z_t \simeq 0.01$  as a possible solution of the Hubble and growth tensions,” *Phys. Rev. D* **104**, L021303 (2021), [arXiv:2102.06012 \[astro-ph.CO\]](https://arxiv.org/abs/2102.06012).
- [62] George Alestas, Lavrentios Kazantzidis, and Leandros Perivolaropoulos, “ $w - M$  phantom transition at  $z_t < 0.1$  as a resolution of the Hubble tension,” *Phys. Rev. D* **103**, 083517 (2021), [arXiv:2012.13932 \[astro-ph.CO\]](https://arxiv.org/abs/2012.13932).